SAND2016-7977C

Performance and Reliability of PV Inverter Component and Systems due to Advanced Inverter Functionality

Jack Flicker and Sigifredo Gonzalez

Sandia National Laboratories, Albuquerque, NM 87185, USA

***Abstract* — In order to identify reliability issues associated with advanced inverter operation and array states (e.g. volt-VAR control, high DC/AC ratios), we have collected system and component-level electro-thermal information in a controlled laboratory environment under both nominal and advanced functionality operating conditions. The results of advanced functionality operation indicated increased thermal and electrical stress on components, which will have a negative effect on inverter reliability as these functionalities are exercised more frequently in the future.**

***Index Terms* —Advanced Inverter Functionality, BOS, PV Reliability**

I. INTRODUCTION

As of 2013, the installed cost of residential PV systems was $4.69/Watt [1]. While most research, both historically and currently, focuses on the production costs of PV module technology, the cost of the necessary BOS components has been largely ignored. As the price of PV modules drops, the price of BOS becomes more important. BOS now constitute 8-12% of the total lifetime PV cost [2]. As of 2010, the inverter and associated power conditioning components accounted for $0.25/Watt [3], well above the DOE benchmark of $0.12/Watt by 2020. As efforts to lower PV module costs yield diminishing returns, the importance of understanding and lowering BOS costs become an increasingly critical and cost effective investment towards achieving the DOE SunShot goals.

One of the key price drivers of power electronics is reliability [4, 5]. PV modules have long lifetimes with warranties offered up to 20 years. In utility-scale fielded systems, the mean time between failure of inverters has been shown to be 300 to 500 times shorter than modules [6, 7]. In one 27-month study, module failures accounted for only 5% of total energy losses, while inverter failures accounted for 36% of lost energy over the same period [8].

The inverter is a challenging reliability target because it is a complicated switching/monitoring system with a number of responsibilities. In addition to providing output power meeting power quality standards, the inverter may also be required to manage power output of the PV module, connect/disconnect from the grid, read and report status, or monitor islanding [2]. Meanwhile, trends in power electronics systems and devices over the last decade have placed increasing demands on the efficiencies of the thermal management and control systems used for MOSFET and IGBT modules. The pressure to decrease the size of power electronics systems and inverter sub-systems has resulted in an overall 50% foot print area reduction of many IGBTs over the last 10 years [9].

This has resulted in higher dissipation requirements for the IGBT die and adjacent inverter components (e.g. capacitors, inductors) due to an increase in die and inverter-system topology densities [10]. In addition, industry increased trends in IGBT switching frequencies, voltage ratings and non-unity power factor (PF) operations of inverters have also resulted in higher heat dissipation levels and temperature-related degradation that directly impacts reliability.

Of special concern are additional inverter functionalities (Fig. 1) and PV array states (e.g. volt-VAR, high DC/AC ratios), which were not envisioned for inverters made as few as five years ago. The new functionalities are pushing the operational limits inverters were designed for, increasing stress on internal components. This is expected to have a significant effect on the reliability and lifetime of inverters. For example, the average capacity factor of a PV power plant have been shown historically to be around 13-20% depending on technology and geography [11, 12]. As advanced inverter functionality increases, this capacity factor will increase towards 100% as power plant operators provide volt-VAR support to the grid during all hours of the day in order to maximize revenues. If a plant operator were to increase the capacity factor to 100% by providing volt-VAR support 24 hours a day, the inverter would see a 5-8x increase in usage/stress. This would decrease the lifetime of the inverter and historical MTBFs of 1-15 inverter-years [6, 7] could theoretically decrease to as low as 0.125-1.875 inverter-years.

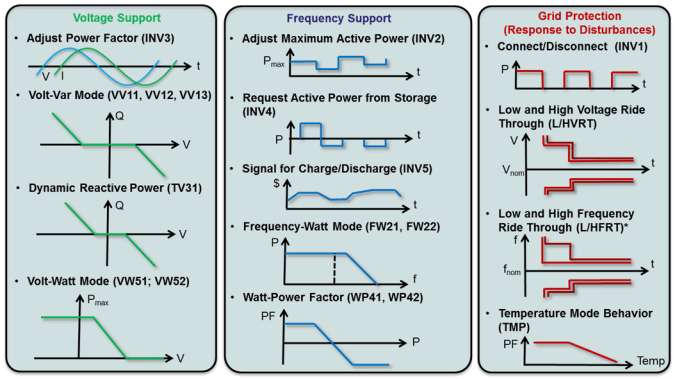

Fig. 1: Autonomous advanced inverter functionalities as defined by IEC TC 61850-90-7 (with the exception of frequency ride through) [13].

II. EXPERIMENTAL

A. *Non-unity Power Factor Operation*

Future markets will incentivize operators to utilize the inverter up to its full power-rating for all daytime hours at various PFs, subjecting the inverter to much higher losses over its operational life and, inevitably, resulting in shorter lifetimes. Since inverters do not need to be exporting any active power, it is also conceivable for an inverter to source/sink VARs 24 hours a day. The newest generation of inverters on the market has taken the first steps required to make continuous VAR support a possibility [14].

Voltage and current waveforms of MOSFET switches were recorded simultaneously along with system-level information during unity and non-unity operation in a 3 kW residential inverter. MOSFET voltage and current were measured over an entire 16 ms AC cycle with temporal resolution of 2-4 ns for power factor operations ranging from -0.85 (current lags voltage) to +0.85 (current leads voltage). In order to correlate the losses in the MOSFET to losses in the system as a whole, system-level efficiency as well as temperatures at eight different positions in the inverter cabinet were monitored and logged at one and five second intervals, respectively.

MOSFET voltage was monitored via Tektroniks voltage probes with drain-source current measured via a mini Rogowski coil. To minimize variations in the readings, DC power was provided by an Ametek PV simulator while AC output was dissipated by an AC simulator. Tests were conducted at PV input powers of 2.81 and 3.29 kW provided by 14 Sanyo HIT 200 and 44 Astro-Power 75 simulated modules, respectively. Electrical data was collected via an Agilent DPO 3014 oscilloscope and analyzed with MATLAB. Temperature data was taken with K-type thermocouples using a Campbell Scientific data logger.

During each switch transition, the MOSFET voltage and current are both non-zero and overlap, which leads to an increase in power dissipation. If the instantaneous power is averaged over the sampling time and summed, the cumulative energy loss as a function of power factor can be quantified. The time duration of the switching transient, where the power is non-zero, is dependent on the power factor of inverter operation, which leads to changes in energy losses and system efficiency.

This procedure was carried out over a number of different power factors, and the cumulative energy loss is clearly a function of inverter operation conditions (
Fig. 2, top) with switching energy losses per cycle increasing by 168% from unity to PF=+0.8275. The losses shown in
Fig. 2 (top) are only from switching losses, since the conduction and diode losses were cancelled out via baselining. However, the non-switching loss mechanisms show the same trend with regard to PF operation with larger losses occurring at higher leading power factors.

It is important to note from
Fig. 2 that higher input power levels yield higher losses in the MOSFETs. It is also interesting to note that the losses are not symmetric around unity power factor operation (even though the operational voltages and currents handled by the MOSFET are). Leading PF operation has much higher losses than lagging operation. This may possibly be due to filtering choices made by the manufacturer.

For larger deviations from unity, the changes in system efficiency can become quite large. One inverter that operates at 96% efficiency at unity PF will drop to 91.3% efficiency at 0.55 PF. This doubling of energy loss will have a significant effect on component operating temperature and will substantially reduce component lifetime.

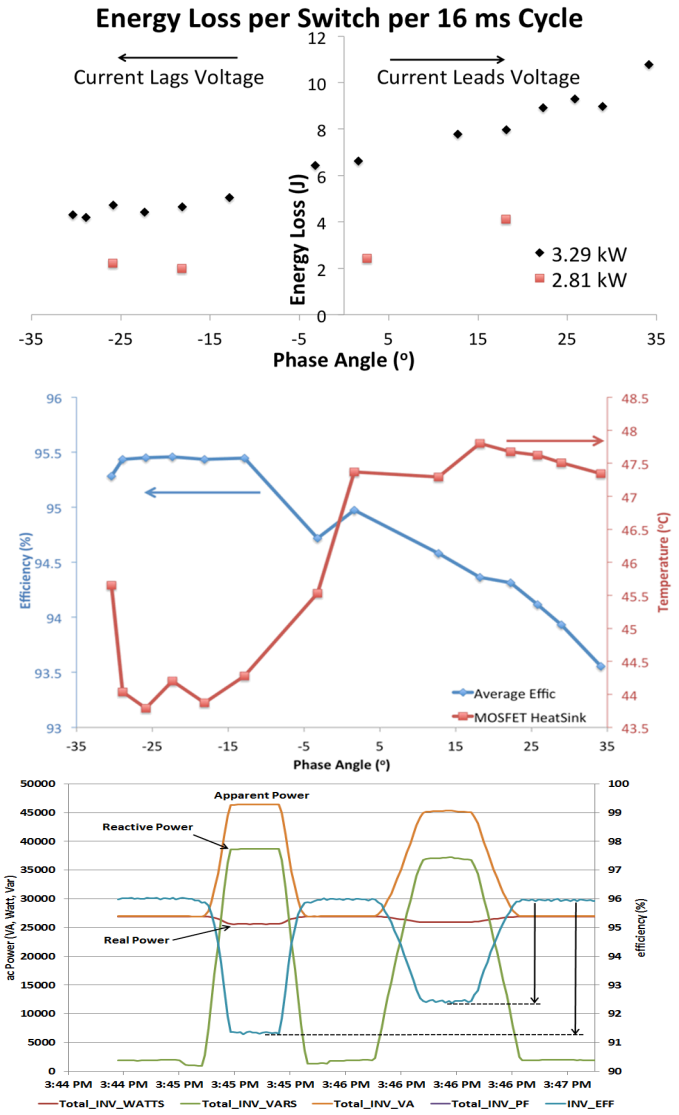

Fig. 2: Non-unity PF operation can have a significant effect on component and system losses. (Top) Total energy loss per 16 ms cycle per switch for different PFs and input powers. (Middle) System-level efficiency (blue) and temperature of MOSFET heat-sink (red) during PF operation. (Bottom) System efficiency for high PF operation (~0.5).

B. Low-Voltage Ride-through

The large-scale penetration of variable and intermittent distributed resources into the electrical grid can have significant effects on frequency and voltage stability of the grid. It is predicted that as penetration ratios increase [15, 16], the number and severity of grid parameter deviations from nominal will also increase (especially far away from distribution feeders).

Historically, distributed generation has had such a low penetration ratio that, in low-voltage events, PV inverters have been asked to disconnect from the grid in order to prevent an islanding situation from occurring (since removing the active power of a small numbers of inverters on the grid was not sufficient to exacerbate the voltage deviation). However, as the penetration ratio increases and the power generated by distributed resources becomes non-negligible, PV inverters that disconnect from the grid can exacerbate the voltage deviations, decreasing grid reliability issues in the future. Therefore, new rules, such as the California Public Utility Commission's (CPUC) Rule 21 interconnect requirements, are being implemented which demand that inverters ride-through a low (or high) voltage event. In Hawaii, where upwards of 12% of households have rooftop solar, the ride through requirements had to be expanded due to the larger voltage fluctuations on the island grid (which has significantly less inertia than other grids) [17].

In the future, as the number of distributed resources on the grid increases, the frequency of voltage excursion may increase. Thus, the increased losses of a PV inverter during a ride-through event may become a non-negligible aspect to the unit reliability over its lifetime.

In the new interconnection requirements, the voltage level of the ride through event determines the mode of operation of the inverter. For example, for Rule 21, in the event of a voltage sag lower than 0.5 PU (V_{sag} > 0.5 PU), the device under test must cease to energize and ride through the voltage sag for a duration of 1 second. If the voltage recovers above 0.5 PU within 1 second, then the inverter must resume energizing the utility up to 90% of pre-event power level within 1 second. An example of an inverter riding through in this manner is shown below (Fig. 3).

During the ride through event, the ac current has a 36% transient spike and the dc voltage experiences a 24.3% voltage transient as the DC bus immediately returns to open circuit. During the low grid voltage condition, the inverter ceases to energize the utility. When the grid voltage returns to nominal, the dc voltage experiences a ringing transient voltage waveform. This ringing results in an increase in bus voltage above open circuit, to 500 V, which applies additional voltage stress to the DC-side components. After this transient, the inverter commences to return to its previous operating conditions and commences maximum power point tracking and power export.

A residential inverter with EPS support capability was evaluated in a laboratory setting to investigate possible stresses on the dc and ac components and any adverse effects of the performance of the inverter when the inverter goes through a grid voltage anomaly. The inverter analyzed has L/HVRT capabilities, but does not adhere to Rule 21 requirements due to the lack of a momentary cessation function.

Voltage and current waveforms of MOSFET switches were recorded simultaneously along with system-level information in a 3 kW residential inverter during low voltage ride through events ranging from 0-1.5 s with V_{sag} ranging from 0-220 V. MOSFET voltage was monitored via Tektroniks voltage probes with drain-source current measured via a mini Rogowski coil. To minimize variations in the readings, DC power was provided by an Ametek PV simulator. Grid transients were simulated using a California instruments RS90 grid simulator. Tests were conducted at PV input powers of 3.29 kW provided by 14 Sanyo HIT 200 and 44 Astro-Power 75 simulated modules, respectively. Electrical data was collected via an Agilent DPO 3014 oscilloscope and analyzed with MATLAB.

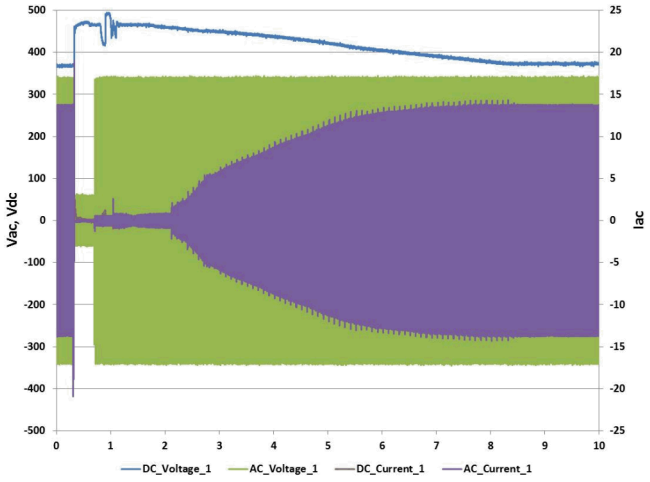

Fig. 3: System voltages and current from a LVRT event

Cumulative MOSFET switching loss during each voltage transient event was calculated and then normalized by the duration of the event in order to determine the relative severity of the LVRT event. The results of normalized energy loss per switch as a function of ride through time and V_{sag} are shown in Fig. 4 and Fig. 5, respectively.

As can be seen from Fig. 4, the rate of energy loss during the event is independent of event length with a value of approximately 682±40 J/s. This indicates that for all LVRT events the inverter attempts to export energy. Since the inverter in question does not adhere to Rule 21, it never enters the "cease to energize" state (0-0.5 PU for t_{event} < 1 s, shown by the dashed blue line) nor does it disconnect when the ride through event is longer than 1 s. Such behavior would be evident from Fig. 4. Since, at 0.195 PU, the corresponding Rule 21 behaviors are "momentary cessation" and

"disconnect", the normalized energy loss of a Rule 21 compliant inverter would be close to zero.

For the residential inverter studied, the rate of energy loss during an LVRT event is linearly related to the value of V_{sag} (Fig. 5) with a maximum normalized energy loss equal to 879 J/s for V_{sag} = 0V. The energy loss decreases at a rate of approximately -3.5 J/V as V_{sag} increases until the energy loss is zero at a PU of unity. Each of the ride through events represented in Fig. 5 has a duration greater than 1 s. This means that to be Rule 21 compliant, the inverter should cease to export power and for all V_{sag}< 0.5 PU (120 V), shown as the solid blue line. So a Rule 21 inverter should have a linear increase in normalized energy loss until 0.5 PU. For V_{sag} < 0.5 PU, the normalized energy loss should be nearly zero due to the "momentary cessation" operation mode.

Based on the data presented here, it is apparent that an inverter that rides through a low voltage event experiences increased losses compared to normal operation. The new CPUC Rule 21 interconnection requirements, especially the "momentary cessation" operation mode, will tend to decrease the LVRT losses of inverters for voltage transients below 0.5 PU.

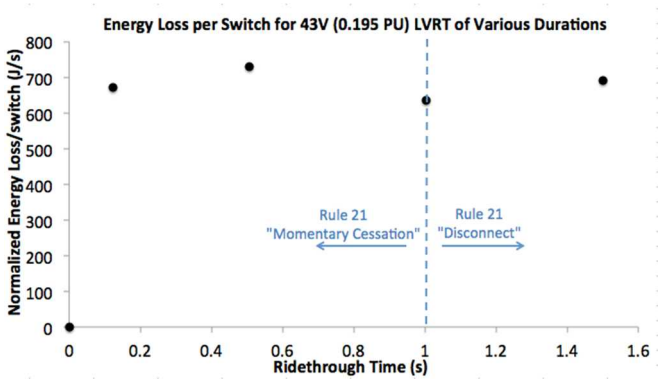

Fig. 4: Normalized energy loss per switch for LVRT events (V_{sag}=43 V) of different durations from 0-1.5 s. The energy loss per switch is independent of ride-through time, indicating that the inverter is actively exporting energy for all LVRT events.

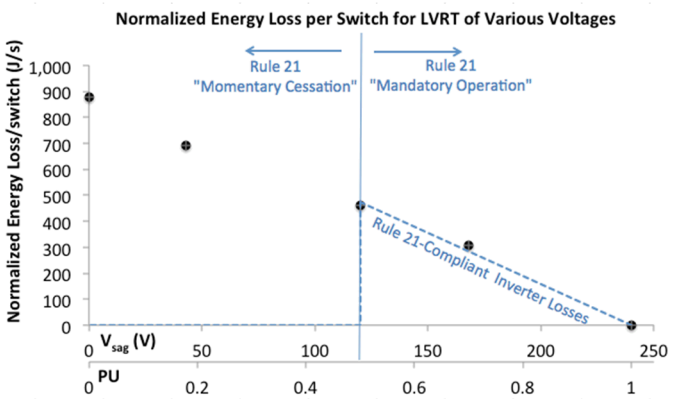

Fig. 5: Normalized energy loss per switch for LVRT events of different V_{sag} values from 0-240 V with durations of 1-1.5 s (in the "cease to energize" regime for V_{sag}=0-120 V).

CONCLUSIONS

In general, from emergence over the past five to its eventual large-scale implementation on the electric grid in the coming years, advanced inverter functionalities look to enable even higher penetration of renewable energy generation through the stabilization of grid voltage and frequency and mitigation of renewable energy variability and uncertainty. However, it must be noted that these advanced operational modes increase power system losses and will lead to shorter unit lifetimes. It is necessary to consider the balance of added grid stability with the shorter lifetimes of the units that will result, especially as these functionalities become more monetized in the future as grid support markets continue to evolve and inverters are asked to exercise these functions on a much more regular basis.

ACKNOWLEDGEMENTS

This work was funded by the DOE Office of Energy Efficiency and Renewable Energy. Sandia National Laboratories is a multi-program laboratory managed and operated by Sandia Corporation, a wholly owned subsidiary of Lockheed Martin Corporation, for the U.S. Department of Energy's National Nuclear Security Administration under contract DE-AC04-94AL85000.

REFERENCES

[1] D. J. Feldman, G. Barbose, R. Margolis, T. James, S. Weaver, N. Darghouth, R. Fu, C. Davidson, S. Booth, and R. Wiser, "Photovoltaic System Pricing Trends," National Renewable Energy Laboratory, PR-6A20-62558, 2014. Available: http://www.nrel.gov/docs/fy14osti/62558.pdf

[2] Y. Xue, K. C. Divya, G. Griepentrog, M. Liviu, S. Suresh, and M. Manjrekar, "Towards Next Generation Photovoltaic Inverters," 2011 IEEE Energy Conversion Congress and Exposition (ECCE), 2011.

[3] L. Bony, S. Doig, C. Hart, and E. Maurer, *Achieving low-cost solar PV: Industry Workshop Recommendations for Near-term Balance of System Cost Reductions*: Rocky Mountain Institute (RMI), 2010.

[4] A. Ristow, M. Begovic, A. Pregelj, and A. Rohatgi, "Development of a Methodology for Improving Photovoltaic Inverter Reliability," *IEEE Transactions on Industrial Electronics,* vol. 55 (7), pp. 2581-2592, Jul 01 2008.

[5] B. Jablonska, H. Kaan, M. Leeuwen, and G. Boer, "PV-prive Project at ECN: Five Years of Experience With Small-scale AC Module PV Systems," *Presented at the 20th European Photovoltaic Solar Energy Coference and Exhibition,* 2005.

[6] A. Maish, "Defining Requirements for Improved Photovoltaic System Reliability," *Progress in Photovoltaics,* pp. 165-173, 1999.

[7] A. B. Maish, C. Atcitty, S. Hester, D. Greenberg, D. Osborn, D. Collier, and M. Brine, "Photovoltaic System Reliability,"

Conference Record of the Twenty Sixth IEEE Photovoltaic Specialists Conference, 1997, 1997.

[8] A. Golnas, "PV System Reliability: An Operator's Perspective," *Photovoltaics, IEEE Journal of,* vol. 3 (1), pp. 416-421, 2013.

[9] S. G. Leslie. (2006) Cooling Options and Challenges of High Power Semiconductor Modules. *Electronics Cooling*. Available: http://www.drymaxxair.com/uploads/Cooling Options And Challenges of Semiconductor Modules.docx

[10] P. Wang, P. McCluskey, and A. Bar-Cohen, "Two-Phase Liquid Cooling for Thermal Management of IGBT Power Electronic Module."

[11] J. Apt and A. Curtright, "The spectrum of power from utility-scale wind farms and solar photovoltaic arrays," 2008.

[12] Renewable Energy Massachusetts LLC. (2013). *Massachusetts: A Good Solar Market* [Microsoft PowerPoint Presentation]. Available: http://www.remenergyco.com/wp-content/uploads/2010/05/CONFIDENTIAL_Renewable_Energy_Massachusetts_Executive_Summary_April_20_2010.ppt

[13] International Electrotechnical Commission (IEC) Technical Report 61850-90-7, "Communication networks and systems for power utility automation –Part 90-7: Object models for power converters in distributed energy resources (DER) systems." Geneva, Switzerland, 2013.

[14] "Q at Night: Reactive power outside of feed-in operation," Dec 22 2014. Available: http://www.sma.de/fileadmin/Partner/SMA_Connect/WP_QATNIGHT.AEN132110W.pdf

[15] R. Passey, T. Spooner, I. MacGill, M. Watt, and K. Syngellakis, "The potential impacts of grid-connected distributed generation and how to address them: A review of technical and non-technical factors," *Energy Policy,* vol. 39 (10), pp. 6280-6290, 10// 2011.

[16] M. A. Eltawil and Z. Zhao, "Grid-connected photovoltaic power systems: Technical and potential problems—A review," *Renewable and Sustainable Energy Reviews,* vol. 14 (1), pp. 112-129, Jan 2010.

[17] P. Fairley. (5 Feb 2015) 800,000 Microinverters Remotely Retrofitted on Oahu—in One Day. *IEEE Spectrum*. Accessed: http://spectrum.ieee.org/energywise/green-tech/solar/in-one-day-800000-microinverters-remotely-retrofitted-on-oahu.